Journal of Computational Neuroscience manuscript No.
(will be inserted by the editor)

Learning Neural Connectivity from Firing Activity: Scalable Algorithms with Provable Guarantees

Amin Karbasi · Amir Hesam Salavati · Martin Vetterli

Received: date / Accepted: date

Abstract

The connectivity of a neuronal network has a major effect on its functionality and role. It is generally believed that the complex network structure of the brain provides a physiological basis for information processing. Therefore, identifying the network's topology has received a lot of attentions in neuroscience and has been the center of many research initiatives such as Human Connectome Project. Nevertheless, *direct* and invasive approaches that slice and observe the neural tissue have proven to be time consuming, complex and costly. As a result, the *inverse* methods that utilize firing activity of neurons in order to identify the (functional) connections have gained momentum recently, especially in light of rapid advances in recording technologies; It will soon be possible to simultaneously monitor the activities of tens of thousands of neurons in real time.

While there are a number of excellent approaches that aim to identify the functional connections from firing activities, the scalability of the proposed techniques plays a major challenge in applying them on large-scale datasets of recorded firing activities. In exceptional cases where scalability has not been an issue, the theoretical performance guarantees are usually limited to a specific family of neurons or the type of firing activities.

In this paper, we formulate the neural network reconstruction as an instance of a graph learning problem, where we observe the behavior of nodes/neurons (i.e., firing activities) and aim to find the links/connections. We develop a scalable learning mechanism and derive the conditions under which the estimated graph for a network of Leaky Integrate and Fire (LIF) neurons matches the true underlying synaptic connections. We then validate the performance of the algorithm using artificially generated data (for benchmarking) and real data recorded from multiple hippocampal areas in rats.[1]

Keywords Functional connectivity · Synaptic connectivity · Neural signal processing · Neural network

Amin Karbasi
Inference, Information and Decision Systems Group
Yale Institute for Network Science
Yale University
New Haven, U.S.A.
E-mail: amin.karbasi@yale.edu

Amir Hesam Salavati
Laboratory of Audiovisual Communications (LCAV)
School of Computer and Communication Sciences
Ecole Polytechnique Federale de Lausanne (EPFL)
Lausanne, Switzerland
E-mail: hesam.salavati@epfl.ch

Martin Vetterli
Laboratory of Audiovisual Communications (LCAV)
School of Computer and Communication Sciences
Ecole Polytechnique Federale de Lausanne (EPFL)
Lausanne, Switzerland
E-mail: martin.vetterli@epfl.ch

1 Introduction

Reconstructing the connectivity of neuronal networks has been a major challenge for the past decade. Currently, the only reliable way to map the underlying *synaptic connectivity* of neuronal networks is by using invasive procedures, which are prohibitively complex and time-consuming: it took more than 10 expert/year to map the whole connectome of *C. Elegans*, comprising only 302 neurons and 7283 synaptic connections (Watts and Strogatz, 1998). Similarly, a 10 expert/year effort was required to capture the connectome of *fruit fly* medulla columns, with only 379 traced neurons and 8637 synapses (Plaza et al, 2014). To map the whole brain of a fruit fly, with around $10,000$ neurons, we would have to spend around 4700 expert/year (Plaza et al, 2014; Chiang et al, 2011). Following the same approach and using the current technology, it is estimated that it will take around 14 billion man/year to completely map the human brain's connectome (Plaza et al, 2014). Although there is an increasing effort to make some parts of the invasive procedures automated, such approaches remain impractical even

[1] The code and the data related to this paper is available at `http://rr.epfl.ch/paper/KSV2016`

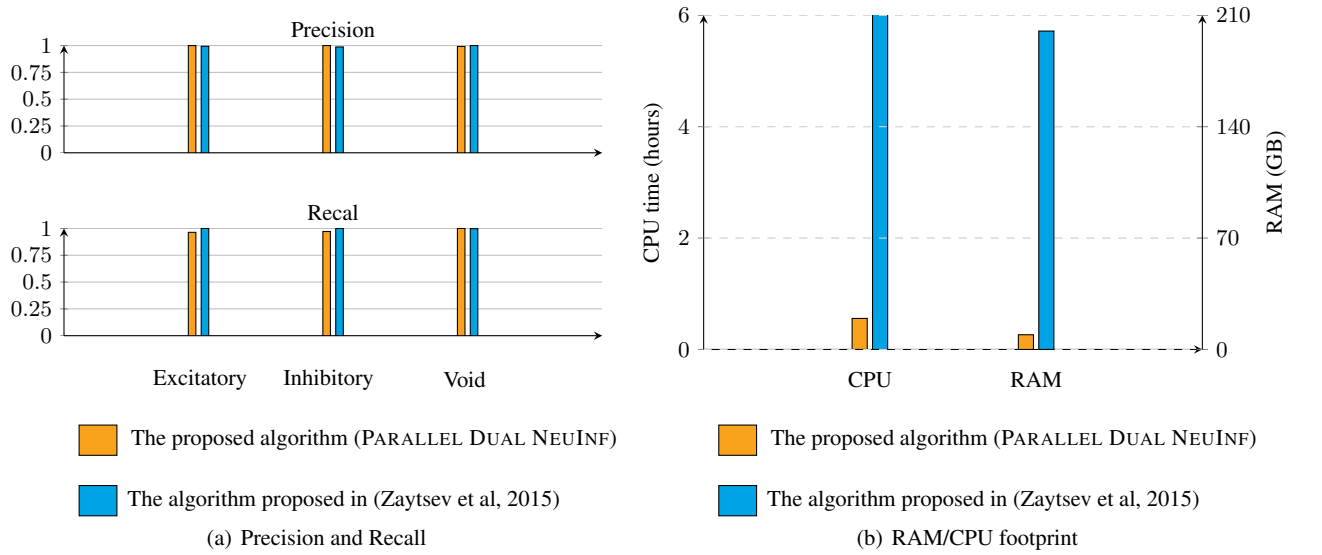

(a) Precision and Recall

(b) RAM/CPU footprint

Fig. 1: Performance of our proposed algorithm in identifying the *type* of neural connections in a network of 1000 LIF neurons for a dataset of artificially generated spiking activities (courtesy of Zaytsev et al (2015)) **(a)** and the memory/CPU footprint of our proposed algorithm compared to a similar approach proposed in Zaytsev et al (2015) over the same dataset.

for mid-sized networks. Furthermore, the current invasive techniques cannot be applied to live specimen.

In contrast, *inverse* methods with the focus on mapping the *functional* connectivity from the activity of the neurons have received more attention in recent years. These approaches are non-invasive (or minimally invasive) so they can be applied to live specimen and they require much less time and labor to identify the functional network. Furthermore, rapid advances in recording technologies has made it possible to simultaneously monitor the activities of tens (Perin et al, 2011) to hundreds of neurons (Buzsáki, 2004; Grewe et al, 2010). Upcoming technologies will significantly improve the accuracy and scale of recording neurons' activities. It is worth mentioning that there has also been significant progress in simultaneously recording and stimulating a set of neurons (Khodagholy et al, 2014; Herrera and Adamantidis, 2015; Bertotti et al, 2014). These advancements provide an abundance of data for which computationally efficient and accurate inverse algorithms would be welcome.

In this paper, we focus on the inverse problem. Our main goal is to design efficient and *scalable* algorithms that result in good approximations of the underlying *synaptic graph*. In other words, we are interested in algorithms whose inferred functional network is a close match to that of the underlying synaptic connectivities for a group of Leaky Integrate-and-Fire (LIF) neurons (Gerstner and Kistler, 2002).

To this end, we apply a technique, usually known as the *kernel method* in the machine learning literature, to map the nonlinear inference problem to a linear equivalent in the kernel space. Then, we formulate the network inference problem as an instance of a constrained optimization problem where the objective function has a simple form and the constraints are all linear. As a result, we develop an algorithm that easily scales to large datasets of recorded neural activities. Moreover, we theoretically study this mapping and derive the conditions under which our proposed algorithm successfully identifies the *type* of underlying synaptic connections (e.g. being excitatory/inhibitory) in the limit of large available data.

We also show that the proposed technique is equally applicable to networks of both deterministic or stochastic neurons that follow the widely used LIF model. We support our theoretical findings with an exhaustive set of simulations where we validate the performance of our algorithm with respect to the ground truth networks (in artificially generated spiking data where the ground truth is available). We also report the result of our algorithm applied to a datatset of firing activities recorded from hippocampal areas in rats Mizuseki et al (2013). We find that our results are quite in line with previous findings (Mizuseki et al, 2009).

Figure 1 summarizes the main contributions of this paper in a nutshell: in Figure 1(a) we show that in the limit of large data, the proposed algorithm can successfully identify the type of synaptic connections, whereas Figure 1(b) demonstrates the memory/CPU footprint of the proposed approach compared to that of the approach based on Generalized Linear Models (GLM) (Zaytsev et al, 2015).[2]

[2] We sincerely thank Dr. Yury Zaytsev, Prof. Abigail Morrison and Dr. Moritz Deger for making their data and code publicly available.

2 Related Work

Cross Correlogram is perhaps the most widely-used method to identify (functional) connection between pairs of neurons or regions (Brown et al, 2004). However, approaches based on Cross Correlogram usually fall short of identifying *causal* relation or *effective* connectivity of neurons. It is very well established in statistics that the existence of correlation between two events is neither a necessary nor a sufficient conditions for inferring causality. This is why statistical hypothesis tests such as *Granger causality measure* were proposed as an alternative in order to overcome the drawbacks of Cross Correlogram (for instance, see the work of Kim et al (2011)).

Another recent line of work has primarily focused on inference methods that are tailored to LIF model of neurons. In particular, Van Bussel et al (2011) convert the non-linear firing behavior of LIF neurons into a set of linear equations, which can be solved given a sufficient number of recorded samples. While being efficient, this algorithm is highly sensitive to the accuracy of spike times and relies on the knowledge of model parameters (e.g. synaptic propagation delays) which are difficult to obtain. Memmesheimer et al (2014) proposed an inference algorithm based on the Perceptron learning rule, similar to Baldassi et al (2007), for which they proved that under accurate estimate of spike times it is possible to identify a simple n-to-1 feed forward network. They also proposed a heuristic extension that works with *finite precision* in recorded spike times. Nevertheless, their model does not take the (random) synaptic delays into account. Moreover, having extra post-synaptic neurons even in a simple feed forward scenario can have a dramatic effect on the performance of the inference algorithm when the structure of the graph (i.e., here being feed-forward) is not known a priori.

A more complex and accurate family of approaches rely on Generalized Linear Models (GLM) (Paninski, 2004). These methods consider the collective activity of the neural group and focus on finding the best functional network that can explain the traffic. GLM was recently used in reconstructing a real physiological circuit from recorded neural data (Gerhard et al, 2013) as well as reconstructing the functional connectivity for the ganglion cells in the retina (Pillow et al, 2008). The approaches that are based on GLM are generally accurate (i.e. they identify the correct set of connections in the underlying graph) *provided* that the neural model used to generate the spike data matches exactly the one used in GLM (Ramirez and Paninski, 2014). Extending these methods to exploit the prior distribution on the neural connections results in effective Bayesian models that are especially powerful in the face of limited data. In particular, Stevenson et al (2009) proposed a Maximum a Posteriori (MAP) estimate to infer the neural connections and reported highly accurate results in limited data regime at the expense of very high computational costs. Bayesian approaches have also been used in identifying connections directly from calcium-imaging data (Mishchenko et al, 2011).

In light of the aforementioned advantages, GLM-based techniques are among the favorite state-of-the art approaches. Nevertheless, they are not without limits. The first and probably most important drawback is scalability, which makes handling large datasets, both in terms of number of neurons and duration of recorded firing activity, difficult. Recently, however, several approximations have been suggested to resolve this issue (Ramirez and Paninski, 2014; Zaytsev et al, 2015). Nevertheless, these approximations work only for a particular choice of nonlinearity (Zaytsev et al, 2015) and similar to GLM-based techniques, the convergence is only guaranteed when the model for neurons and that of GLM's closely match each other.

In this paper, we propose a novel approach in identifying the functional connections which offers the following properties:

1. **Scalability**: from a practical point of view, it allows more scalability, i.e. it requires less memory and can scale with limited resources available (see Figure 1).
2. **Performance guarantees**: from a theoretical point of view, its performance guarantees hold under a larger family of neurons and nonlinearities.
3. **Hidden neurons**: the simplicity of the approach also enables us to derive the sufficient conditions under which the estimated functional network returned by our algorithm is not affected by the existence of hidden neurons and matches the underlying synaptic skeleton in the limit of large data.

Finally, we should mention that the *consistency problem* even for a n-to-1 feed forward network is NP-hard. In words, determining whether or not there exists a set of delays and weights such that we can fully match the set of input firing patterns to the output is very difficult (Maass and Schmitt, 1999) . Although this result does not necessarily imply that finding such a configuration is impossible (under the right set of conditions), it shows that finding provable "positive learning results" for the case of spiking neurons is quite challenging.

3 Model Formulation and Problem Statement

We formally introduce the neural models and the network structures considered throughout the paper. We also formally state the network inference problem.

Neurons' model: We first consider a network of *deterministic* but *noisy* Leaky Integrate and Fire (LIF) neurons (Gerstner and Kistler, 2002) with a *fixed* firing threshold θ. In this

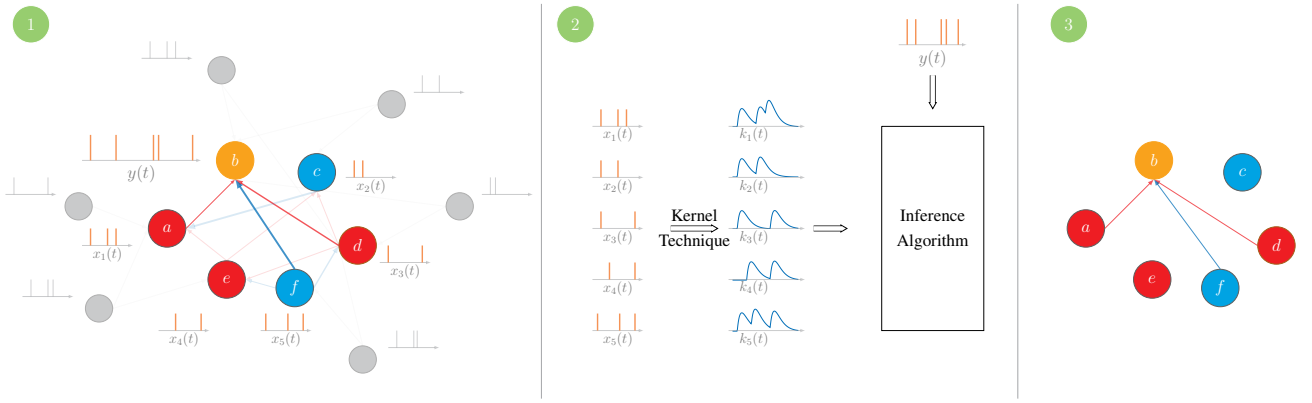

Fig. 2: Network model: a recurrent neural network where we try to identify the incoming connections of node b by observing the spike trains $x_1(t), \ldots, x_5(t)$ and $y(t)$. Here we assume that edges have randomly chosen propagation delays and neurons can be excitatory or inhibitory. Note that there are some "hidden" neurons (shown in gray) in the network as well and whose spiking activities are not recorded but they affect the membrane potential of the observed neurons. After applying some "kernel" to account for the integration and leak in the membrane potential, we look for the set of weights that result in the best prediction of the output firing pattern, $y(t)$. The result will ideally be as shown in Part 3. Note that in this paper we are not interested in reconstructing the exact weights (shown in Part 1 through the thickness of the lines), but to tell if two neurons are connected to each other and, if so, what the connection type is. If we repeat these steps for the incoming connections to other neurons, which can be done in parallel, we will get the complete connectivity graph.

model, the membrane potential of a given neuron at time t is described by

$$h(t) = h_0 + \sum_{i=1}^{n} g_i K_i(t) + v(t), \tag{1}$$

where h_0 is the baseline voltage, g_i is the actual synaptic weight (i.e. the ground truth) of the incoming connection from the pre-synaptic neuron i, $K_i(t)$ is the accumulated effect of neuron i on the post-synaptic neuron at time t, and $v(t)$ is an additive "noise" (the noise term can be the result of different parameters, such as thermal fluctuations).

The form of $K_i(t)$ in Eq. (1) depends on the choice of the *kernel* (or filter) for the membrane potential of the considered post-synaptic neuron. For instance, if we choose an exponentially decaying filter, then

$$K_i(t) = \sum_{t_f \in \mathcal{T}_i, t_f \leq t - d_i} e^{-\frac{t - t_f - d_i}{\tau_m}}, \tag{2}$$

where τ_m is the membrane time constant, d_i is the propagation delay between neuron i and the post-synaptic neuron and $\mathcal{T}_i$ is the set of firing times for the pre-synaptic neuron i.

The output, also called the *activity*, of the post synaptic neuron at time t will be

$$y(t) = f(h(t) - \theta),$$

where $f(\cdot)$ is the Heaviside step function and θ is the firing threshold. We also assume that after a firing, the membrane potential is *reset* back to the resting potential h_0.

Another model of neurons that we also consider in this paper is the *stochastic* LIF model where the membrane potential is explained by Equation (1) as before but the post-synaptic neuron's activity is stochastic and is given by the following probability:

$$\Pr\{y(t) = 1\} = f_s(h(t) - \theta). \tag{3}$$

Here, $f_s(\cdot)$ is *an increasing* function of its argument. There are several choices for $f_s(\cdot)$ proposed in the literature in which the logistic function is perhaps one of the most popular. In this paper, however, we do not specify a particular function and only require that the function $f_s(\cdot)$ is increasing in its argument.

Network model: As for the network structure, we do not assume any specific topology on the neural graph. However, as is the case in many neural networks, we require a *balanced* network in terms of excitatory and inhibitory connections. This requirement ensures that the excitatory and inhibitory population act in such a way that the average activity stays below a threshold.

In that regard, we usually pick 80% of connections to be excitatory and 20% to be inhibitory. For numerical results, we set the weights of all excitatory connections to be $+1$mV and that of an inhibitory connection to $-\delta$mV, where $\delta = n_{exc}/n_{inh}$, and n_{exc} and n_{inh} are the number of excitatory and inhibitory connections in the network. Also, in accordance with biological data and following Dale's principle Dale (1935), we fix the type of neurons to be either

excitatory or inhibitory, which means all outgoing connections of a pre-synaptic neuron have the same sign.

We also assume that neural connections have intrinsic delays which represent the time it takes for the information to propagate through the axons and synapses. The delay for each link is assumed to be a random number in the interval $(0, d_{\max}]$, where $d_{\max} > 0$ is the maximum delay. The delays do not change, once assigned, they remain fixed.

Problem Statement: The goal of this paper is to propose a scalable learning algorithm that infers the (functional) *connectivity matrix* only by observing the firing activity of the neurons. Ideally, such an algorithm should be able to explain the observed firing activity as accurately as possible. Furthermore, we study conditions under which the identified functional connectivity is a close approximation of the underlying synaptic connectivity. Specifically, we would like to design algorithms in order to identify the *type* of neural connections. In other words, the inference algorithm should be able to find out if neuron i has a directed connection to neuron j, and if so, whether the connection is excitatory or inhibitory. Figure 2 illustrates the model and the problem considered in this paper.

4 The Inference Algorithms

We propose an iterative inference algorithm to identify the functional connections in a network of neurons based on their firing activity. To better explain the algorithm, we first study the simpler case of deterministic LIF neurons, as described in Eq. (1). We then show in a later section that how the proposed algorithm can be naturally extended to deal with stochastic neurons as well.

To start, let us assume that we are interested in identifying the incoming connections to one post-synaptic neuron (e.g. neuron b in Figure 2). The following procedure can be then applied to every single neuron. In that case, note that we can re-write Equation (1) in a vector form as

$$u = Kg + v, \tag{4}$$

where $u_{T\times 1}$ is a vector whose t-th entry is $u_t = h(t) - h_0$, K is a $T \times n$ matrix whose (t,i)-th entry is $K_{ti} = K_i(t)$, $g_{n\times 1}$ is the vector of actual synaptic connection weights (i.e. $g = [g_1, \ldots, g_n]^\top$) and $v_{T\times 1}$ is the noise vector (i.e. $v = [v(1), \ldots, v(T)]^\top$). Without loss of generality, we assume $h_0 = 0$ and $\theta = 0$[3]. Now, let us define

$$\hat{y}(t) = \begin{cases} +1 \text{ if } y(t) = 1; \\ -1 \text{ if } y(t) = 0; \end{cases} \tag{5}$$

where $y(t)$ is the state of the post-synaptic neuron at time t. This way, we know that

$$K_t g + v(t) \geq 0, \ \forall t : \hat{y}(t) > 0$$

and

$$K_t g + v(t) \leq 0, \ \forall t : \hat{y}(t) < 0,$$

where K_t is the t-th row of matrix K. By letting $\hat{Y}_{T\times T} = \text{diag}(\hat{y}(1), \ldots, \hat{y}(T))$, we can rewrite the above constraints in a matrix form as follows:

$$\hat{Y}(Kg + v) > \mathbf{0}, \tag{6}$$

where $\mathbf{0}$ is the all zero vector and the inequality is entrywise. Equation (6) is the cornerstone of our proposed algorithm. In order to find the neural connections, we aim to solve the following optimization problem

$$\textbf{\textit{Problem I}:} \ \min_w \|w\|_\ell \quad \text{s.t.} \quad \hat{Y}K'w > \mathbf{0}. \tag{7}$$

Basically, by knowing the matrix $\hat{Y}$ and the firing activity of neurons, we will look for the smallest vector vector w (in ℓ-norm) that satisfies a set of constraints. Also note that we used a different kernel matrix K', which may or may not be the same as the true kernel matrix K, depending on our *prior knowledge* about the underlying neural model.

We will show that in scenarios where the original problem is feasible, i.e. when $Kg > \mathbf{0}$, as long as K' and K are close (in some precise algebraic sense) then by solving *Problem I*, given by Equation (7), we will be able to find the type/sign and the location of non-zero entries in g, the vector of the underlying synaptic neural connections.

In practice, however, due to incoming traffic from hidden neurons as well as large membrane noise, *Problem I* may be infeasible, i.e. the constraints define an empty set. Therefore, to design a more practical algorithm we reformulate the problem as follows:

$$\textbf{\textit{Problem II}:} \ \min_w \|w\|_\ell + \sum_t L(A_t w), \tag{8}$$

where A_t is the t-th row of matrix A, defined as $A = \hat{Y}K'$, and L is a convex loss function that penalizes unsatisfied constraints. This way, we look for a regularized solution w^*. Note that for a proper choices of ℓ (e.g. $\ell \geq 1$), the above problem is convex.

There are many choices of loss functions used in the literature. One of the most well-known is hinge-loss, i.e.,

$$L(x) = \max(0, 1 - x).$$

For the rest of the paper, we will use hinge loss as well since it has been well-studied in machine learning algorithms and there is a wealth of optimization techniques for efficiently solving the above optimization problem.

[3] Both these terms can be easily integrated into the weight vector by appending a separate entry to the vector g and the kernel matrix K. We focus on the case where $\theta = h_0 = 0$ for simplicity.

4.1 Centralized Inference Algorithms

There is a wealth of possible algorithms to solve *Problem II*, given by Equation (8). Here, we propose two different *online* approaches, with emphasis on scalability and capability to deal with limited memory.

The first approach is an extension of the Perceptron-based algorithm we proposed in (Karbasi et al, 2015) and focuses on solving the primal problem. In the proposed approach, we choose $\ell = 1$ to favor sparsity in the connections. Then, by noting that the sub-gradient of the hinge loss function is

$$L'(x) = \begin{cases} -1 \text{ if } L(x) > 0; \\ 0 \quad \text{otherwise;} \end{cases}$$

we derive the following update rule at iteration τ of the algorithm:

$$w(\tau + 1) = w(\tau) + \gamma L(A_i w(\tau)) A_i^\top,$$

where γ is the learning rate.

Now, to take care of the sparsity regularization, let $\mathcal{F}(x, \eta)$ be the following soft-thresholding function

$$\mathcal{F}(x, \eta) = \begin{cases} x - \eta \text{ if } x > \eta, \\ x + \eta \text{ if } x < -\eta, \\ 0 \qquad \text{if } |x| < \eta. \end{cases} \tag{9}$$

Previous studies have shown that iteratively applying the soft-thresholding function above to our estimates $w(\tau)$ will result in a sparse solution (Wright et al, 2009), (Goldstein et al, 2014). As a result, and by putting these steps together, the proposed approach, called NEUINF, is shown in Algorithm 1.

Algorithm 1 NEUINF

Input: The observations matrix A over period T, a maximum number of iterations S, sparsity threshold η, learning rate γ, initial vector $w(0)$.
Output: Connections belief vector w
  for $\tau = 1 \to S$ **do**
    Pick $i \in \{1, ..., T\}$ at random
    Set $\hat{w}(\tau) = w(\tau) + \gamma L(A_i w(\tau)) A_i^\top$,
    Set $w(\tau + 1) = \mathcal{F}(\hat{w}(\tau), \eta)$.
  end for
  Return $w(S)$.

The second approach is based on solving the *dual* form of *Problem II* using the (Stochastic) Dual Coordinate Descent method. This particular formulation is specially interesting from the scalability viewpoint, as discussed in (Jaggi et al, 2014). To this end, and to facilitate the formulation, we choose $\ell = 2$ in this approach and use the soft-threshold function to trim the entries of the returned weight vector. To formulate the problem in its dual form, we use Fenchel's conjugate of the loss function and the regularization term. The Fenchel dual of the ℓ_2-norm is itself and that of the hinge loss is given by

$$L^\star(x) = \begin{cases} x \quad \text{if } -1 < x < 0; \\ \infty \text{ otherwise.} \end{cases}$$

Therefore, we can formulate the dual problem as (Jaggi et al, 2014):

$$\begin{aligned} \max_{\lambda \in [0,1]^T} E(\lambda) &= -c\|A^\top \lambda\|_2^2 - \sum_t L^\star(-\lambda_t) \\ &= -c\|A^\top \lambda\|_2^2 + \sum_t \lambda_t, \end{aligned} \tag{10}$$

where $\lambda_{T \times 1}$ is the vector of the dual variables and c is a positive constant to control the extent of regularization. By solving the above problem for the optimal dual variables, λ^*, we can then find the optimal set of weights as

$$w^* = A^\top \lambda^*. \tag{11}$$

We can solve *Problem II* using the Stochastic Dual Coordinate Descent (SDCD) technique. The details are given in Algorithm 2. One strong point of the coordinate descent method is that it does not require a step size (learning rate) and, therefore, does not require tuning. This make it particularly attractive from the practical point of view.

Algorithm 2 DUAL NEUINF

Input: The observations matrix A over period T, a maximum number of iterations S,sparsity threshold η, initial vectors $w(0)$ and $\lambda(0)$.
Output: Connections belief vector w
  for $\tau = 1 \to S$ **do**
    Pick $i \in \{1, ..., T\}$ at random
    Set $\Delta\lambda = \text{argmin}_{\Delta\lambda + \lambda_i \in [0,1]} c\|w(s) + A_i \Delta\lambda\|_2^2 - (\lambda_i + \Delta\lambda)$
    Set $\hat{w}(\tau) = w(\tau) - \Delta\lambda A_i^\top$,
    Set $w(\tau + 1) = \mathcal{F}(\hat{w}(\tau), \eta)$.
    Set $\lambda_i(\tau + 1) = \lambda_i(\tau) + \Delta\lambda$.
  end for
  Return $w(S)$ and $\lambda(S)$.

4.2 Scalable Inference Algorithms

In practical situations, the matrix of observed neural activity could be very large, especially due to the large number of recorded samples, T. For instance, one of the datasets that we have used to evaluate the performance of the proposed algorithm has around $T = 7,000,000$ rows and $n = 1000$ columns, i.e. a matrix of size 7000000×1000. In some cases the dataset will be even larger. Fitting such large matrices into memory (RAM) is usually difficult due the limited amount of available resources. Therefore, it is desirable to design an algorithm that can cope with the limits on memory. Furthermore, from the computational point

of view, it would also be important to have an algorithm that can break the problem into smaller sub-problems, solve those sub-problems *in parallel*, and merge the results such that the overall solution is optimal.

To this end, we have also designed parallel versions of NEUINF and DUAL NEUINF that can deal with limited memory and to fully utilize the available computational resources. We first divide the data matrix into M non-overlapping smaller blocks $A^{(1)}, \ldots, A^{(M)}$, each of size (around) $T/M \times n$. We can then apply either Algorithm 1 or Algorithm 2 to solve the inference problem for each block and later merge the results. Depending on the amount of available resources, we either can do this process in parallel (i.e. if enough RAM is available) or do this process sequentially, loading one block $A^{(i)}$ at a time into the memory (i.e. when RAM is limited). The proposed computational architecture is shown Figure 3.

The detailed process for parallelizing NEUINF is given in Algorithm 3. For algorithms that are based on Dual Coordinate Descent methods, e.g. Algorithm 2, an elegant parallelization procedure is proposed in Jaggi et al (2014), called Communication-Efficient Distributed Dual Coordinate Ascent (CoCoA). We will adapt this technique to parallelize DUAL NEUINF. The details are shown in Algorithm 4.

Algorithm 3 PARALLEL NEUINF

Input: The observations matrix A over period T, a maximum number of iterations S,sparsity threshold η.
Output: Connections belief vector w
  Initialize $w(0) = (0, \ldots, 0)_{1\times n}$
  for $s = 1 \rightarrow S$ **do**
    Initialize $\Delta w = [0, \ldots, 0]_{n\times 1}$
    for Each Block $m = 1 \rightarrow M$ (and in parallel if possible) **do**
      Let $z = \text{NEUINF}(A^{(m)}, w(s))$
      $\Delta w = \Delta w + z$
    end for
    $w(s) = w(s-1) + \frac{\Delta w}{M}$
  end for

Algorithm 4 PARALLEL DUAL NEUINF

Input: The observations matrix A over period T, a maximum number of iterations S,sparsity threshold η.
Output: Connections belief vector w
  Initialize $w(0) = (0, \ldots, 0)_{1\times n}$
  for $s = 1 \rightarrow S$ **do**
    Initialize $\Delta w = [0, \ldots, 0]_{n\times 1}$
    for Each Block $m = 1 \rightarrow M$ (and in parallel if possible) **do**
      Let $z, \Lambda = \text{DUAL NEUINF}(A^{(m)}, w(s), \lambda^{(m)}(s))$
      $\Delta w = \Delta w + z$
      $\lambda^{(m)}(s) = \lambda^{(m)}(s-1) + \frac{\Lambda}{M}$
    end for
    $w(s) = w(s-1) + \frac{\Delta w}{M}$
  end for

5 Theoretical Analysis

In this section, we analyze the performance of the proposed algorithms in order to identify connections under which the returned functional graphs closely approximates the underlying synaptic connections.

We start by proving the desired results for a neural network consists of deterministic (and noisy) LIF neurons specified by Equation (1). We also assume that there is incoming traffic from some unobserved (also called *hidden*) neurons. We establish sufficient conditions on both statistical properties of the noise as well as the *inference kernel* (denoted by K') such that the type of connections in identified functional graph by the algorithms introduced in the previous section matches the type of corresponding neural connections in the underlying synaptic graph. We then extend our results to show that the same algorithm can be applied to the more realistic scenario of *stochastic* LIF neurons.

5.1 Network of Deterministic Noisy LIF Neurons with Hidden Traffic

For the network of deterministic noisy LIF neurons, we first show that as long as the noise term satisfy some statistical properties, the algorithm yields the desired result. We then investigate the conditions under which the net effect of incoming traffic from a set of hidden neurons can be modeled by the noise term with the specified statistical properties, which means that the algorithm will be successful in identifying the connection types even in presence of unobserved traffic.

To start, let us remind ourselves that the membrane potential of LIF neurons, define in Equation (1), is given by

$$h(t) = h_0 + \sum_{i=1}^{n} g_i K_i(t) + v(t),$$

where $v(t)$ is the added noise at time t. Intuitively, if the magnitude of noise is very small, then the set of constraints $\hat{Y}Kg > \mathbf{0}$ will not be affected by noise. Likewise, if the noise has a zero mean, and we have enough firing data for the pre-synaptic neurons, we should be able to reconstruct the connections on average and in the limit of large data.

The following assumptions state the above intuition more rigorously. We then show that as long as these assumptions are held, we can identify the type of connections in the limit of large T.

(A1) **Having enough firing data**: the observed neurons fire at a rate linear T, i.e. neuron i fires $\alpha_i T$ spikes in the interval $[0, T]$, with $\alpha_{\min} > 0$.

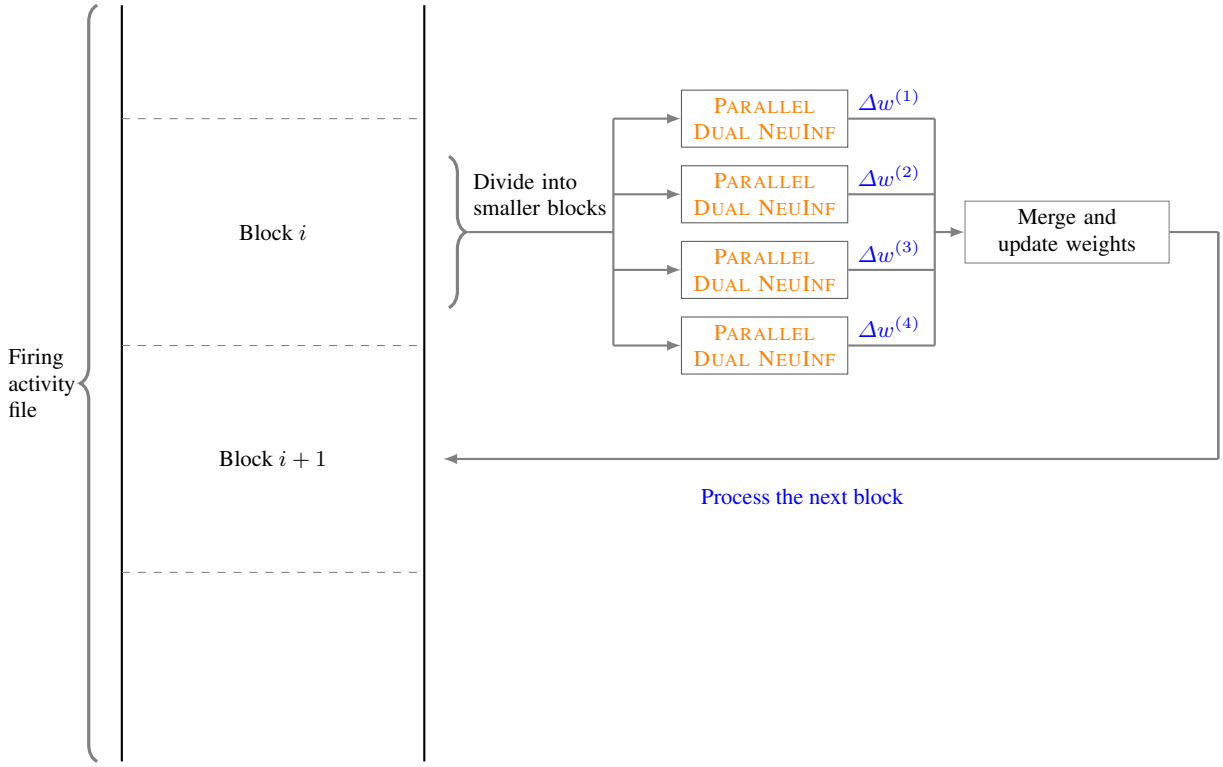

Fig. 3: Parallelization architecture.

(A2) **Zero-mean noise**: the noise in the membrane potential $\{v(t)\}$ is a zero-mean[4] random variable and its samples are uncorrelated if they are more than Δ_v time slots apart.

Note that the first assumption makes sure that each neuron fires enough spikes for its connection to be successfully identified and the second assumption basically states that the noise should have a *vanishing correlation*, i.e. the very long future samples should not depend on the current samples. We also trivially pick the inference kernel K' in such a way that it proportionally captures the quantity of the firing activity, i.e. the entries in the inference kernel matrix, K' are non-negative and the number of non-zero entries in column i of the matrix K' is proportional to the number of spikes fired by neuron i.

With the above assumptions in mind, we can prove the following lemma.

Lemma 1 *Let us assume that we have enough samples such that the matrix $K^\top K$ and $(K')^\top K'$ are invertible. Now, if the matrix $K^\top K'$ is positive definite, then, under the assumption A1-A2 defined above, and in the limit of large T, we can recover the type of the actual connections, i.e., the estimated weight vector w^* (the output of Algorithm 1 or 2) has the same sign as the actual connection weights, namely,*

$$\lim_{T\to\infty} Pr\{w_i^* g_i > 0\} \to 1,\ \forall i = 1, \dots, n,\ \textit{where}\ |g_i| \neq 0.$$

(The proof is given in Appendix A.1) The above theorem addresses the case of a deterministic noisy LIF neuron. Now we can use this result and extend it to a scenario where we have incoming traffic from a set of unobserved (hidden) neurons. To this end, suppose there are m unobserved neurons whose spikes affect the membrane potential of the post-synaptic neuron in consideration through a set of connections $g' = [g'_1, \dots, g'_m]$. As a result, we can rewrite Equation (4) as,

$$u = Kg + Hg', \tag{12}$$

where $H_{T\times m}$ is the net effect of m outside neurons filtered through the neural kernel. Now, given the result of Lemma 1, we intuitively know that as long as Hg' is a zero-mean random variable with vanishing correlation, we should be able to recover the type of connections. The following assumptions formulate this intuition more rigorously.

(A3) Traffic of two hidden/outside neurons i and j are independent of each other.

[4] Even if the noise has a non-zero mean, it might be possible to compensate for that by adjusting the firing threshold in such a way that the mean of noise remain zero.

(A4) The incoming weights from the hidden/outside neurons form a *balanced random* network (similar to the incoming traffic from "visible" neurons), i.e.,

$$\mathbb{E}\{g_i'\} = 0.$$

(A5) Outgoing traffic of neuron i at time t and $t + \Delta$ are uncorrelated for sufficiently large Δ.

In words, assumptions A3 and A4 ensure that Hg' is a zero-mean random variable with vanishing correlation. Assumption A5 requires that the firing activity of each neuron has *vanishing correlation*, i.e. very far ahead future spikes should be uncorrelated from current spikes. Out of the three, assumption A3 is probably the most strict one and assumption A5 is the weakest one as it is automatically satisfied when there is a *post-synaptic* spike in the interval $[t, t + \Delta)$ (due to the "reset" effect of the membrane potential).

Note that a direct consequence of the above assumptions is that if we sample constraints at intervals that are far apart, the noise terms should be uncorrelated. This might become handy in practice to design better algorithms.

Now the following theorem shows that given the above assumptions, we can rewrite Hg' as a zero-mean colored noise with vanishing correlation.

Lemma 2 *Given assumptions A2-A5 above, the random variable $v(t) = H_t g'$ form a colored random variable with vanishing correlation.*

(The proof is given in Appendix A.2) Combining the results of Lemma 1 and Lemma 2, we can prove the convergence of the algorithm for the case of deterministic noisy LIF neurons with incoming hidden traffic. This is formally proven in the next theorem.

Theorem 1 *Let us assume that we have enough samples such that the matrix $K^\top K$ and $(K')^\top K'$ are invertible. Now, if the matrix $K^\top K'$ is positive definite, then, under the assumptions A1 through A5 stated above, and in the limit of large T, we can recover the type of the actual connections, i.e., the estimated weight vector w^* has the same sign as the actual connection weights. formally,*

$$\lim_{T\to\infty} Pr\{w_i^* g_i > 0\} \to 1,\ \forall i = 1, \ldots, n,\ \textit{where}\ |g_i| \neq 0.$$

(The proof is given in Appendix A.3)

5.1 Network of Stochastic LIF Neurons

In the previous section, we proved that under certain assumptions the proposed algorithms are guaranteed to identify the type of connections in the limit of large data for deterministic LIF neurons (with hidden incoming traffic as well). In this section, we show that the same can be proved for stochastic LIF neurons if we slightly modify the proposed algorithm. The main idea is to show that solving the problem for stochastic neurons results in the same solution as solving the problem for deterministic neurons, defined in *Problem II*. Therefore, we can solve *Problem II* for the stochastic case as well to identify the connections.

To start, recall that the firing rule for stochastic LIF neurons, defined in Equation (3) is given by

$$\Pr\{y(t) = 1\} = f_s(h(t) - \theta),$$

where the membrane potential, $h(t)$ is given by

$$h(t) = h_0 + \sum_{i=1}^{n} g_i K_i(t) + v(t),$$

Now from a statistical point of view, we can cast the neural network reconstruction as an instance of a Maximum Likelihood estimation: find a vector w that maximizes the likelihood of observing the output spike pattern $\{y(t)\}$, given the set of pre-synaptic spikes or their "filtered" effect through the kernel matrix K'. More precisely,we are interested in solving the following problem:

$$\arg\max_{w} \Pr\{y|K', w\}, \tag{13}$$

where y is the $T \times 1$ vector of observed post-synaptic spikes and K' is the $T \times n$ neural kernel matrix that captures the leaky integrated effect of the pre-synaptic neurons. This is in fact what traditional GLM approaches do to identify the vector w (Paninski, 2004). However, in this section, we show that under mild and natural assumptions on the post-synaptic neuron and its firing pattern, solving Problem (13) is equivalent to solving *Problem II*. By establishing this connection we can solve the above ML problem at scale, as we explained earlier.

The assumptions are as follows

(B1) The function $f_s(\cdot)$ is an increasing function of its argument.

(B2) The firing pattern of the post-synaptic neuron has a *vanishing correlation*, i.e., if two samples are more than Δ time slots apart, they becoming conditionally independent. More precisely, if $t' - t > \Delta$, then

$$\begin{aligned}\Pr\{y(t), y(t')|K', w\} &= \Pr\{y(t)|K'(0,t), w\} \\ &\quad \times \Pr\{y(t')|K'(t,t'), w\},\end{aligned}$$

where $K'(t_1, t_2)$ is the subset of samples in the interval $[t_1, t_2]$.

Note that Assumption A2 will be easier to satisfy if the post-synaptic neuron has fired at least once in the interval $[t, t')$, due to the *reset* effect of neurons.

Under our assumptions, we know that if we only consider samples that are more than Δ time slots apart, they are independent. With slight abuse of notation, let $y_{T'\times 1}$ and $K'_{T'\times n}$ denote the vector of sampled output spikes that are at

least Δ samples apart and the corresponding kernel matrix, respectively. Then, one can rewrite the ML problem (13) as

$$\arg\max_{w} \Pr\{y|K', w\} = \arg\max_{w} \prod_{t=1}^{T'} \Pr\{y(t)|K'(t), w\} \tag{14}$$

or equivalently,

$$\arg\max_{w} \sum_{t=1}^{T'} \log\left(\Pr\{y(t)|K'(t), w\}\right). \tag{15}$$

Let T'_+ indicate the set of time instances such that $\forall t \in T'_+$ we have $y(t) = 1$. Likewise, let T'_0 be the set of instances such that $y(t) = 0$, for $\forall t \in T'_0$. By combining Equations (1), (3), and (15) we obtain the following optimization problem to solve

$$\arg\max_{w, \|w\|_2=1} \sum_{t\in T'_+} \log\left(f_s(K'_t w)\right) + \sum_{t\in T'_0} \log\left(1 - f_s(K'_t w)\right), \tag{16}$$

where K'_t is the t-th row of K'. To simplify the above equation, let K''_t be a $1\times n$ vector in such a way that the following holds:

$$1 - f_s(K'_t w) = f_s(K''_t w).$$

Remark 1 *For the special case of f_s being the sigmoid function, we have $K''_t = -K'_t$. This is the form that has been considered in GLM (Paninski, 2004).*

Now, let us define a $T' \times n$ matrix H as follows

$$H_t = \begin{cases} K'_t \text{ if } t \in T'_1; \\ K''_t \text{ if } t \in T'_0; \end{cases} \tag{17}$$

where H_t is the t-th row of H. As a result, we can rewrite problem (16) as

$$\arg\max_{w, \|w\|_2=1} \sum_{t} \log\left(f_s(H_t w)\right) \tag{18}$$

Our main observation is that the optimization problem given by Equation (18) and *Problem II* are equivalent, meaning that the maximizer of Equation (18) is also the minimizer of *Problem II*, as long as we pick a loss function that is

- Decreasing, i.e., $L(x) \leq L(y)$ if $x \geq y$.
- Satisfies the inequality $\log(f_s(x)) \leq -L(x)$.

For instance, if $f_s(\cdot)$ is the sigmoid function, then we can pick $L(\cdot)$ to be the sigmoid function or a slightly modified version of the hinge loss, e.g., $L(x) = \max(\epsilon(1-x), 1-x)$, where $0 < \epsilon < 1$ is a small.

Theorem 2 *Under assumptions B1-B2 above, and with a proper choice of loss function, the problem given by Equation (18) and* Problem II *are equivalent in the sense that the solution w^* to* Problem II *is also the maximizer of Equation (18).*

(The proof is given in Appendix A.4) This equivalence has significant consequences. First, we can efficiently find the ML estimator for problem (13). Second, it also suggests that the convergence results for our deterministic algorithm (discussed earlier in this section) also apply to the stochastic family of neurons.

6 Experiments

In this section we validate the performance of the proposed algorithm via numerical experiments on both artificially generated data as well as data recorded from real neurons. For the former, we have used the dataset generated by (Zaytsev et al, 2015).[5] Testing on artificially generated data has an advantage in having access to the underlying synaptic connectivity (ground truth) which allows benchmarking the performance of the proposed algorithm. We have also applied the inference algorithm to a dataset of real recordings from the multiple hippocampal areas in rats (Mizuseki et al, 2013, 2009).[6]

6.1 Results on Simulated Data

The dataset of artificially generated spikes (Zaytsev et al, 2015) contains the firing activity of 1000 *LIF neurons*, with a fixed firing threshold of 20mV and a random (and unknown) synaptic propagation delay of up to 2ms (Zaytsev et al, 2015). The network topology was recurrent and randomly generated.

We apply PARALLEL DUAL NEUINF to the dataset and compare the returned weights for each neuron to the actual ones. We calculate the accuracy of the algorithm in terms of three measures:

1. Spike prediction accuracy: we verify the ability of the algorithm to predict output firing activity of the post-synaptic neuron (i.e. by solving *Problem I*), given the inferred connection weights and the firing activity of its neighbors (when *Problem I* is feasible).
2. Average *quality*: we take an average over all the returned weights for excitatory, inhibitory and void connections

5 We sincerely thank Dr. Yury Zaytsev, Prof. Abigail Morrison and Dr. Moritz Deger for making their data and code publicly available.

6 We sincerely thank Prof. Kenji Mizuseki, Prof. Anton Sirota, Prof. Eva Pastalkova and Prof. György Buzsáki for making the dataset publicly available.

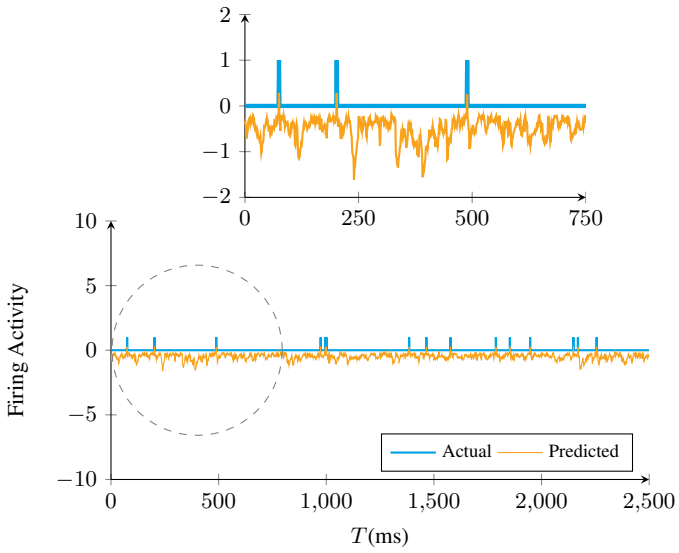

Fig. 4: Sample of predicted vs, observed firing activity for neuron 1 in a recurrent network of 1000 LIF neurons.

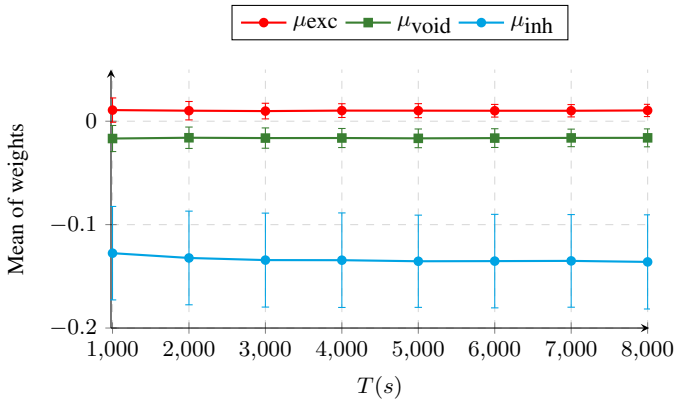

Fig. 5: Average of weights of the incoming connections to neuron 1 returned by Algorithm 2 for each connection type as a function of the total number of recorded samples, T.

when solving *Problem II*. In the ideal case, these three average should be well-separated and the returned weights should be concentrated around the means (i.e., variance should tend to zero).

3. Precision and recall: we then transform the analog association matrix returned by the algorithm to a ternary *adjacency* matrix of the graph. We measure how accurately the algorithm has identified excitatory, inhibitory and void connections by calculating *precision* and *recall* for each connection type.

We start by evaluating the performance of PARALLEL DUAL NEUINF in explaining observed firing activity. For relatively small T, the algorithm is always capable of finding a set of weights that accurately explain the observed activity (since *Problem I* remain feasible). Figure 4 illustrate a sample of observed vs. predicted spike activity by the set of weights returned by Algorithm 2 when the inference kernel K' consists of a single decaying exponential filter with a time constant of 20ms.

Moving to the quality of the returned weights in terms of matching with the underlying synaptic connections, we first calculated the average of returned weights for all excitatory, void and inhibitory connections, respectively. The desired properties that we are looking for are that first there should be an ordering between the average weights (excitatory to be higher than void, and void to be higher than inhibitory). Secondly, the variance of weights for each type should tend to zero as T grows, i.e., the algorithm returns a set of weights where the weights for each connection type are concentrated around their mean. Figure 5 shows that both of the desired properties hold for the proposed algorithm.

We also use the Receiver Operating Characteristic (ROC) curve to evaluate the quality of the returned weights. To this end, we normalize the incoming weights of neurons to zero mean and unit variance. We then gradually adjust two thresholds, one for excitatory and one for inhibitory connections, beyond which we declare a connection excitatory or inhibitory, respectively. For each pair of selected thresholds, the number of true and false positives for each connection type is calculated. The closer the area under the curve is to 1, the better the inference algorithm is. The results for the incoming connections to neuron 1 are shown in Figure 6. As shown in the figure, having more samples result in better inferred graphs. In Figure 6, we also report the ROC curve for the "aggregate inferred weights", where we have performed the inference algorithm 5 times with different hyper parameters and averaged over the results. Clearly, this strategy results in a much better performance and an almost perfect reconstruction of connection types. We can make a trade off between the simulation time and RAM depending on the amount of available resources.

Next, we evaluate the performance of the algorithm in terms of *precision* and *recall*. For this part, we use the aggregate set of weights discussed above and divide the set of incoming connections into three categories (i.e., excitatory, void and inhibitory), using the K-Means clustering algorithm (with 3 clusters). We then count the number of true positive/negatives for each connection type over this ternary adjacency matrix. This way, we can calculate the precision and recall of the algorithm as a function of T for the proposed algorithm, as shown in Figure 7.

We have also examined the effect of hidden neurons on the performance of our proposed algorithm in identifying

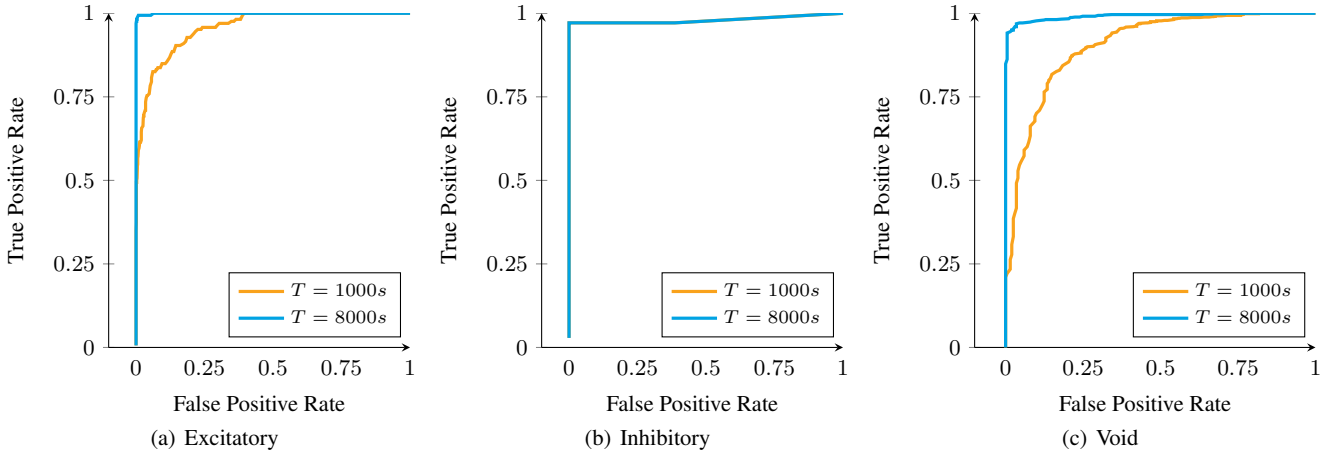

(a) Excitatory (b) Inhibitory (c) Void

Fig. 6: The ROC curve for the incoming connections to neuron 1 returned by Algorithm 2.

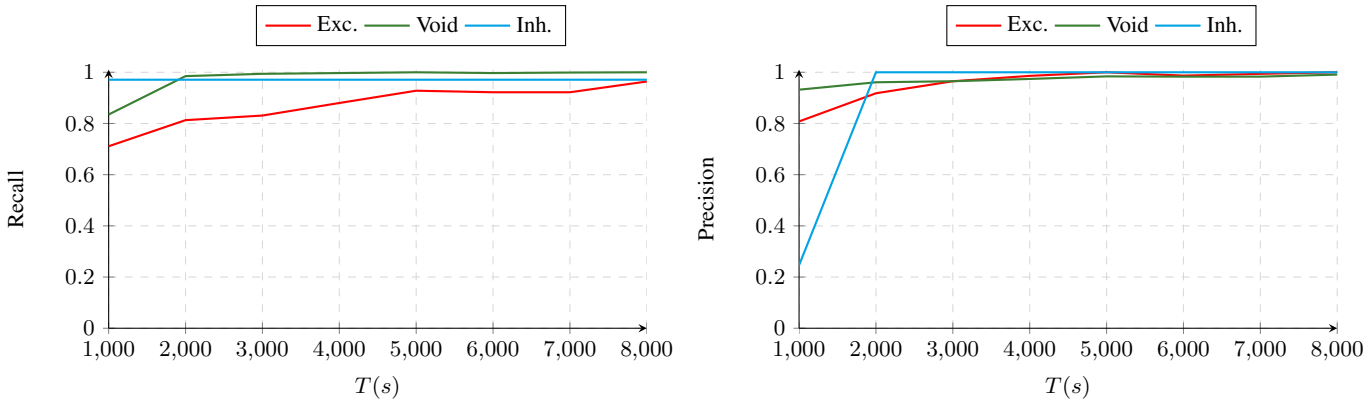

(a) Recall (b) Precision

Fig. 7: Precision and recall of for the incoming connections to neuron 1 in the artificially-generated dataset after transforming the returned association matrix by PARALLEL DUAL NEUINF to a ternary adjacency matrix using the K-Means algorithm. We have averaged over several association matrices before transforming the results to ternary in order to reduce the effect of noise and randomness in the algorithm.

the connection types. Although hidden neurons were also present in the original dataset provided in (Zaytsev et al, 2015), but in order to quantitatively investigate the effect of hidden neurons, we artificially "hid" some neurons in the database by removing their spike times when applying the proposed algorithm. We then evaluated the performance of the algorithm in correctly identifying the type of neural connections among the *visible* neurons. For a fixed number of hidden neurons, we generated 5 random graphs by randomly hiding the given number of neurons. The average results are shown in Figure 8. In the figure, the horizontal axis illustrates the ratio of the number of hidden neurons to the number of visible neurons. The vertical axis show precision and recall for the excitatory, inhibitory and void connections. As shown in this figure, the algorithm is quite robust against the effect of hidden neurons and precision is less affected than recall. In other words, what the algorithm returns is quite accurate, but it might not capture all connections of the specific type when the number of hidden neurons is increasing.

Finally, we calculated the amount of computational resources used by our algorithm. Figure 9 shows the simulation time (in hours) as well as the amount of RAM (in Gigabytes). As expected, since we divide the data matrix into smaller blocks and load them one at a time, the amount of RAM remains fixed and the simulation time scales (almost) linearly with the amount of available data.

6.2 Results on Real Data

After validating the performance of the algorithm on simulated data, we applied the inference algorithm to a dataset of real recordings from the multiple hippocampal areas in rats (Mizuseki et al, 2013, 2009). This dataset corresponds to

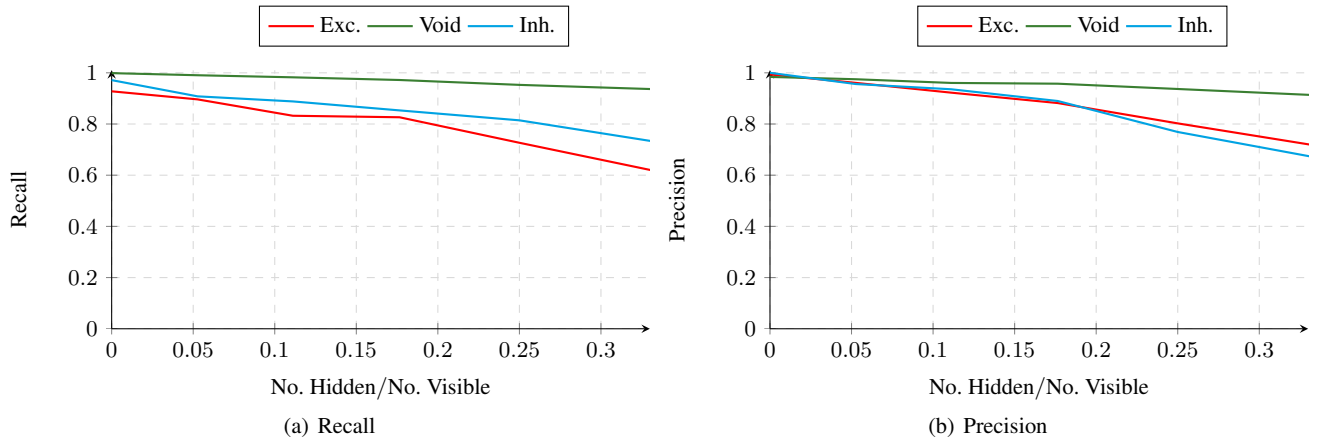

(a) Recall (b) Precision

Fig. 8: Effect of hidden neurons on the precision and recall of for the incoming connections to neuron 1 in the artificially-generated dataset. The horizontal axis shows the ration between the number of hidden and visible neurons in the network.The vertical axes show precision and recall, calculated after transforming the returned association matrix by PARALLEL DUAL NEUINF to a ternary adjacency matrix using the K-Means algorithm.

442 recording sessions when the rats were performing some tasks. In each session, the activity of tens of neurons were recorded simultaneously (ranging from 64 to 256 neurons). Here, and for most of available datasets of recordings from living species, the ground truth is not available. Therefore, we cannot benchmark the performance of the algorithm with respect to the underlying synaptic connectivity. Nevertheless, we can *analyze* the results in order to make sure that they are in line with biological findings about the species and perform sanity checks on the obtained functional graph. With this in mind, Figure 10 illustrates the inferred weights by Algorithm 2 for neuron 1 based on the recordings for task "ec013.18" in the dataset, that contains the firing activity of 94 neurons.

Furthermore, given that the data providers have performed some physiological analysis to determine the type of each neuron (i.e. being excitatory or inhibitory), we have compared the "verdict" of our algorithm about the type neurons against the one found by the data providers. Note that there are several ways of deciding about the "type" of a neuron in our algorithm:

- One can calculate the "net" outgoing weight for each neuron and if it is higher/lower than a threshold, call it excitatory/inhibitory.
- Alternatively, one can count the number of positive and negative "peaks" among the outgoing weights and classify the neuron as excitatory/inhibitory if these two numbers are significantly different from each other.

We considered the second method and the results are shown in Figure 11. To interpret the data given in Figure 11, note that not all neurons were classified in Mizuseki et al (2009) and we only compare the types for neurons that were indeed classified. In the figure, we have also included the results of neuron type prediction using cross correlation that was performed in Mizuseki et al (2009). As shown in Figure 11, the proposed algorithm performs quite well in identifying the excitatory neurons but requires improvements in identifying inhibitory neurons. This might be partly due to the fact that the firing rates of inhibitory neurons in the dataset was on average lower than those of excitatory neurons and the fact that the LIF model we considered in this paper is more accurate in modeling the behavior of excitatory neurons than that of inhibitory ones.

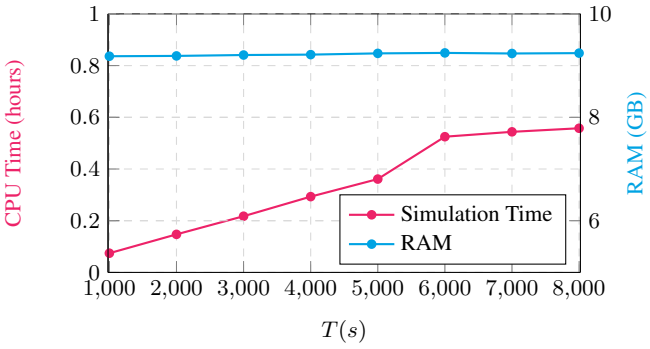

Fig. 9: The amount of CPU and RAM used by the algorithm as a function of T.

7 Conclusion and Future Work

In this paper, we introduced a novel approach to identify neural connectivity from the observed firing activity of neurons. The proposed approach is based on a simplified but

accurate formulation of LIF neurons that facilitates theoretical analysis and allows scalable implementations through machine learning algorithms.

We theoretically proved the accuracy of the algorithm and derived the conditions under which the inferred functional connectivity matches that of the underlying synaptic network. We also showed that the algorithm is capable of dealing with both deterministic and stochastic LIF neurons through the same framework. Finally, using numerical analysis, we showed that the proposed algorithm successfully identifies the synaptic connections over a dataset of simulated spiking activity (to be able to benchmark against the ground truth) and is capable of dealing with datasets of real recordings yielding meaningful interpretations.

As for future directions, there are several major challenges that seems deeply intriguing. The first one concerns the existence of hidden neurons. In this paper we showed that as long as the incoming traffic from hidden neurons satisfy some statistical conditions, we are capable of finding the connectivity for the observed part of the network. Nevertheless, the more interesting challenge would be to (partially) identify the connectivity between the observed and hidden part of the network. The second challenge involves considering more realistic models of neurons. In this paper, we considered LIF neurons with fixed firing threshold. In reality though, the firing threshold is also adaptive and neurons need more accurate models to describe their behavior (especially the inhibitory ones). Taking these dynamical aspects is certainly part of our future work.

Acknowledgements The authors would like to thank Swiss National Science Foundation for supporting this work (grant No. 20FP-1-151073). We also thank Mr. Hesam Setareh, Mr. Mohammad Javad Faraji and Prof. Wulfram Gerstnerfor their kind and helpful discussions on neural models and the proposed approach. We should deeply thank Dr. Yury Zaytsev, Prof. Abigail Morrison and Dr. Mortiz Deger for generously sharing the code and data for their approach on inverse connectivity inference (Zaytsev et al, 2015), as well as Prof. Kenji Mizuseki, Prof. Anton Sirota, Dr. Eva Pastalkova and Prof. György Buzsáki for generously sharing their recorded data from hippocampal areas in rats (Mizuseki et al, 2013, 2009).

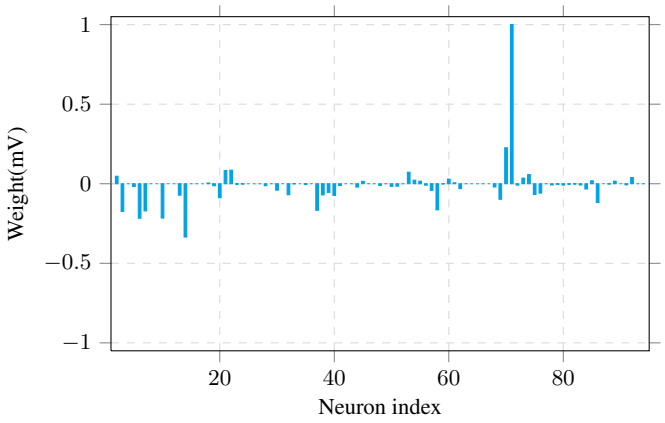

Fig. 10: The incoming connections to neuron 1 in the dataset

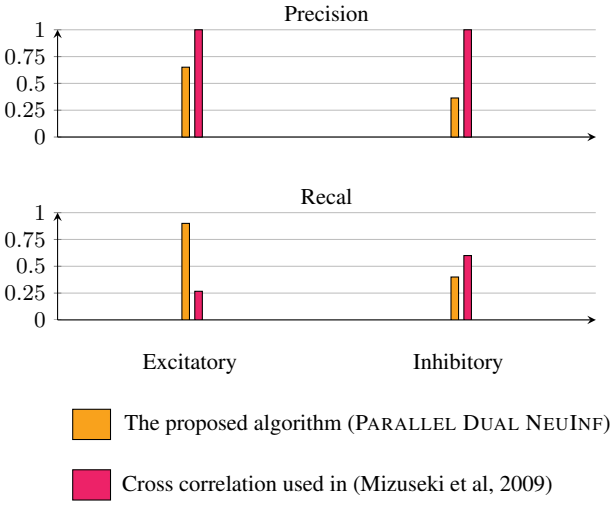

Fig. 11: Comparison of neurons types determined by Algorithm 2 and cross correlation performed in Mizuseki et al (2009). The results are benchmarked against the topological analysis made in Mizuseki et al (2009) to decide the type of the neuron based on physiological evidence. As for the predictions made by Algorithm 2, two different methods are considered for determining the type of a neuron based on its outgoing edges.

Appendix A Proofs of Theorems and Lemmas

Before we proceed to the proofs of the theorems in the paper, we prove a few auxiliary results that will help us obtain the desired proofs.

Lemma 3 *Let r denote a non-zero $1 \times T$ vector and B and E be diagonal matrices with positive diagonal elements. Then, the matrix $Br^\top rE$ is positive semidefinite.*

Proof To start the proof, let $C = r^\top r$. Now, note that $BC = B' \bigodot C$, where $\bigodot$ indicates the Hadamard product and $B' = \mathbf{1}_{T\times 1} b_{1\times T}$, with $b_{1\times T}$ being the diagonal entries of the matrix B. Also, let $E' = \mathbf{1}_{T\times 1} e_{1\times T}$, with $e_{1\times T}$ being the diagonal entries of the matrix E.

Now, matrices B' and E' are positive semidefinite since their only non-zero eigenvalue is equal to the sum of all eigenvalues (the rest are zero), which is equal to the trace of matrix B' (resp. E'), i.e. $\sum_j b_j > 0$ (resp. $\sum_j e_j > 0$).

Furthermore, the only non-zero eigenvalue of matrix C is equal to $rr^\top > 0$, which means matrix C is also positive semidefinite. Also, from Shcur product theorem (Schur, 1911) we know that the Hadamard product of two positive semidefinite matrices is positive semidefinite. Thus, matrix $D = B' \bigodot C = BC$ is positive semidefinite. Likewise, the matrix $D' = D \bigodot E'$ is positive semidefinite, which proves the lemma.

Lemma 4 *Consider a banded matrix H in which only elements that are close the diagonal part are non-zero. More specifically,*

$$H_{ij} = \begin{cases} 0, & \text{if } |i-j| > \Delta, \\ \neq 0, & \text{if } |i-j| \leq \Delta, \end{cases}$$

for some constant integer $\Delta > 0$. Furthermore, let $h = \max_{i,j} |H_{ij}|$. Then,

$$\|H\|_2^2 \leq 8\Delta^2 h^2 = \textit{cons}.$$

Proof To start the proof, let $C = H^\top H$. Then,

$$\|H\|_2^2 = \max_x \|Hx\|_2^2 = \max_x x^\top H^\top H x = x^\top C x \qquad (19)$$

where

$$\|x\|_2 = 1 \qquad (20)$$

Now for matrix C we have

$$C_{ij} = \begin{cases} 0, & \text{if } |i-j| > 2\Delta, \\ \neq 0, & \text{if } |i-j| \leq 2\Delta. \end{cases}$$

As a result, and by letting $x^{(d)}$ be the shifted version of the vector x by d positions to the right and $c = \max_{ij} C_{ij}$, we obtain

$$\begin{aligned} E(x) &= \sum_i \sum_j x_i C_{ij} x_j \\ &= \sum_i x_i \sum_{i-2\Delta \leq j \leq i+2\Delta} C_{ij} x_j \\ &= \sum_i C_{ii}(x_i)^2 + C_{i,i+1} x_i x_{i+1} + \cdots + C_{i,i+2\Delta} x_i x_{i+2\Delta} \\ &\quad + \cdots + C_{i,i-1} x_i x_{i-1} + C_{i,i-2\Delta} x_i x_{i-2\Delta} \\ &\leq c \sum_{d=-2\Delta}^{2\Delta} x^\top x^{(d)} \\ &\leq c \sum_{d=-2\Delta}^{2\Delta} \|x\|_2 \|x^{(d)}\|_2 \\ &\leq 4\Delta c, \end{aligned} \qquad (21)$$

where we have used the fact that $\|x\|_2 = 1$. Therefore,

$$\|H\|_2^2 \leq 4\Delta c. \qquad (22)$$

Now, letting H_i denote the i-th column of H, we obtain

$$c = \max_{ij} C_{ij} = \max_{ij} H_i^\top H_j \leq \|H_i\|_2 \|H_j\|_2.$$

On the other hand, we have

$$\|H_j\|_2 \leq \sqrt{2\Delta h^2}.$$

Therefore, $c \leq 2\Delta h^2$. This implies that

$$\|H\|_2^2 \leq 8\Delta^2 h^2,$$

which concludes the proof.

A.1 Proof of Lemma 1

The proof involves two main steps

1. Showing that mean value of $w_i^* g_i$ (over the noise's probability distribution) is positive.
2. Showing the variance of $w_i^* g_i$ tends to zero as T grows.

To prove the first step, note that from solving *Problem II*, given by (8), we know that there is a vector e with positive entries where the optimal solution, w^*, satisfy (a subset of) the constraints, i.e.,

$$\hat{Y}_c K_c' w^* = e > \mathbf{0}, \qquad (23)$$

where $\hat{Y}_c$ and K_c' correspond to the set of satisfied constraints. As a result, and by letting $F' = (K_c')^{-1}$, we will have

$$w^* = F' E \hat{y}_c,$$

where E is a diagonal matrix with positive entries, i.e., $E = \text{diag}(e)$. Now from Equation (6) we have

$$Kg + v = B\hat{y}, \qquad (24)$$

where B is a diagonal matrix with positive entries. By focusing only on the time instances where w^* satisfy the constraints, we will see that

$$K_c g + v_c = B_c \hat{y}_c,$$

where K_c and B_c are the sub-matrices corresponding to the satisfied constraints. Therefore,

$$g = F(B_c \hat{y}_c - v_c), \tag{25}$$

where $F = K_c^{-1}$. To simplify the notations, let F_i (resp. F_i') denote the i-th row of matrix F (resp. F'). Also, let $C_{T\times T} = F_i^\top F_i'$. As a result, if $g_i \neq 0$, we have

$$\begin{aligned} g_i w_i^* &= (\hat{y}_c^\top B_c - v_c^\top) F_i^\top F_i' E \hat{y}_c \\ &= \hat{y}_c^\top B_c F_i^\top F_i' E \hat{y}_c - v_c^\top F_i^\top F_i' E \hat{y}_c. \end{aligned} \tag{26}$$

Therefore,

$$\begin{aligned} \mathbb{E}\{g_i w_i^*\} &= \hat{y}_c^\top B_c F_i^\top F_i' E \hat{y}_c - \mathbb{E}\{v_c^\top\} F_i^\top F_i' E \hat{y}_c \\ &= \hat{y}_c^\top B_c F_i^\top F_i' E \hat{y}_c, \end{aligned} \tag{27}$$

where the last equality follows from the fact the we had a zero-mean noise. Now from Lemma 3 we know that the matrix $BF_i^\top F_i E$ is positive semidefinite. Therefore,

$$\hat{y}_c^\top B_c F_i^\top F_i' E \hat{y}_c > 0,$$

which means $\mathbb{E}\{g_i w_i^*\} > 0$ if $g_i \neq 0$.[7]

The second part of the proof relies on the fact that the variance of $g_i w_i^*$ tends to 0 as $T \to \infty$. To this end, let Δ_v denote the time window within which the noise term samples in the membrane potential remain correlated. Now, we have

$$\begin{aligned} \sigma^2_{w_i g_i} &= \mathbb{E}\{(w_i g_i)^2\} - (\mathbb{E}\{w_i g_i\})^2 \\ &= \left(\hat{y}_c^\top B_c F_i^\top F_i' E \hat{y}_c\right)^2 + \mathbb{E}\{\left(v_c^\top F_i^\top F_i' E \hat{y}_c\right)^2\} \\ &\quad - 2\mathbb{E}\{\left(\hat{y}_c^\top B_c F_i^\top F_i' E \hat{y}_c\right)\left(v_c^\top F_i^\top F_i' E \hat{y}_c\right)\} \\ &\quad - \left(\hat{y}_c^\top B_c F_i^\top F_i' E \hat{y}_c\right)^2 \\ &= \hat{y}_c^\top E (F_i')^\top F_i \mathbb{E}\{v_c v_c^\top\} F_i^\top F_i' E \hat{y}_c, \end{aligned} \tag{28}$$

where we have used the fact that $\{v(t)\}$ is a zero-mean random variable. Now let $H = \mathbb{E}\{v_c v_c^\top\}$. Then, and using the results of Lemma 4, we will get

$$\begin{aligned} \sigma^2_{g_i w_i^*} &= \hat{y}_c^\top E (F_i')^\top F_i H F_i^\top F_i' E \hat{y}_c \\ &\leq \|H\|_2 \|F_i^\top F_i' E \hat{y}_c\|_2^2 \\ &= \sqrt{8}\sigma^2_{\max} \Delta_v \|F_i^\top F_i' E \hat{y}_c\|_2^2 \\ &\leq \sqrt{8}\sigma^2_{\max} \Delta_v \|F_i^\top F_i'\|_2^2 \|\hat{y}_c\|_2^2 \|E\|_2^2 \\ &= \sqrt{8}\sigma^2_{\max} \Delta_v e^2_{\max} T_c \|F_i^\top F_i'\|_2^2, \end{aligned} \tag{29}$$

where T_c is the number of satisfied constraints (i.e. the length of $\hat{y}_c$), $\sigma^2_{\max}$ is the maximum value in the matrix H and $e_{\max}$ is the maximum entry in the diagonal matrix E. At this point, note that

$$\begin{aligned} \|F_i^\top F_i'\|_2^2 &\leq \|F_i\|_2^2 \|F_i'\|_2^2 \\ &\leq \|F\|_2^2 \|F'\|_2^2 \\ &= \left(\lambda_{\max}(F^\top F)\right)\left(\lambda_{\max}((F')^\top F')\right), \end{aligned} \tag{30}$$

where $\lambda_{\max}(F^\top F)$ is the maximum eigenvalue of the matrix $F^\top F$. Now, since F is the pseudo-inverse of the kernel matrix K_c, we have $F = (K_c^\top K_c)^{-1} K_c^\top$. Therefore,

$$\begin{aligned} \lambda_{\max}(F^\top F) &= \lambda_{\max}(F F^\top) \\ &= \lambda_{\max}((K_c^\top K_c)^{-1} K_c^\top K_c ((K_c^\top K_c)^{-1})^\top) \\ &= \lambda_{\max}((K_c^\top K_c)^{-1}) \\ &= \frac{1}{\lambda_{\max}(K_c^\top K_c)}. \end{aligned}$$

Likewise, we can show that

$$\lambda_{\max}((F')^\top F') = \frac{1}{\lambda_{\max}((K_c')^\top K_c')}.$$

As a result, will obtain

$$\sigma^2_{g_i w_i^*} \leq \frac{\sqrt{8}\sigma^2_{\max} e^2_{\max} \Delta_v T_c}{\lambda_{\max}(K_c^\top K_c)\lambda_{\max}((K_c')^\top K_c')}. \tag{31}$$

We know that for any real-valued symmetric matrix $M_{n\times n}$, we have

$$\forall \nu \in \mathbb{R}^n, \|\nu\|_2 = 1 : \nu^\top M \nu \leq \lambda_{\max}.$$

We set $\nu = \frac{1}{\sqrt{n}}\mathbf{1}_{n\times n}$, and by using $M = K_c^\top K_c$, we get

$$\lambda_{\max} \geq \frac{1}{n}\sum_{ij} M_{ij} \geq \frac{1}{n}\text{Tr}(M),$$

where the last inequality follows from the fact that entries of matrix M (and those of K) are all non-negative. Now we have

$$\begin{aligned} \text{Tr}(M) &= \sum_{i=1}^{n}\sum_{j=1}^{T_c}((K_c)_{ji})^2 \\ &\geq \sum_{i=1}^{n} \alpha_i T_c \\ &\geq \alpha_{\min} n T_c, \end{aligned} \tag{32}$$

where the first inequality follows from the fact that the term $\sum_{j=1}^{T_c}((K_c)_{ji})^2$ is at least as large as the number of spikes fired by neuron i in the interval $[0, T_c]$. Combining the above equations, we obtain

$$\lambda_{\max}(K_c^\top K_c) \geq \alpha_{\min} T_c.$$

Similarly, we can also show that

$$\lambda_{\max}((K_c')^\top K_c') \geq \alpha_{\min} T_c.$$

[7] Note that we have excluded the case where $\hat{y}_c^\top B_c F_i^\top F_i' E \hat{y}_c = 0$ because it will happen if $\sum_t \hat{y}_c(t) = 0$, i.e. if we have the same number of firing instances as the instances of inactivity. However, in real neurons the latter event is much more frequent. Therefore, and when the amount of data increases, the probability of having $\sum_t \hat{y}_c(t) = 0$ tends to zero.

Combined with Equations (28), (29) and (33), this results in

$$\sigma^2_{w_i g_i} \leq \frac{\sqrt{8}\sigma^2_{\max} e^2_{\max} \Delta_v T_c}{(\alpha_{\min} T_c)^2} \leq \left(\frac{2\sigma_{\max} e_{\max}}{\alpha_{\min}}\right)^2 \frac{\Delta_v}{T_c}. \quad (33)$$

This shows the desired result that the variance tends to zero as T_c grows. Given that the number of satisfied constraints also grow with T, the above steps show that the variance tends to zero as T grows.

At this point, and with the above results, we can easily prove the theorem using the Chebyshev's inequality. We simply define $\mu = \mathbb{E}\{g_i w_i^*\}$ and will have

$$\Pr\{|g_i w_i^* - \mu| \geq k\sigma\} \leq \frac{1}{k^2},$$

where $\sigma = \mathbb{E}\{(g_i w_i^*)^2\}$ and k is a constant bigger than one. Now since we know that $\lim_{T\to\infty} \sigma = 0$, we can select the constant k arbitrarily large, which is equivalent to having

$$\lim_{T\to\infty} \Pr\{|w_i^* g_i - \mu|0\} \leq \epsilon, \quad (34)$$

for some arbitrarily small $\epsilon > 0$. This shows that if $g_i \neq 0$, the term $w_i g_i$ will be concentrated around its mean, $\mu > 0$, with probability 1. This proves the theorem.

Remark 2 *Note that the above theorem only states that if there is an underlying synaptic connection, i.e. if $g_i \neq 0$, we will identify its sign in the limit of large data. However, it does not discuss the cases where $g_i = 0$. In those cases, the additional sparsity regularizes (e.g. in the form of ℓ_1-norm minimization) help us prune the connections by removing those that are close to zero.*

A.2 Proof of Lemma 2

We start by calculating $\mathbb{E}\{v(t)v(t-\Delta)\}$ for some integer $\Delta > 0$, noting that $v(t) = \sum_{i=1}^m H_{ti} g'_i$.

$$\begin{aligned}\mathbb{E}\{v(t)v(t-\Delta)\} &= \sum_i \sum_j \mathbb{E}\{H_{ti} H_{t-\Delta,j} g'_i g'_j\} \\ &= \sum_i \mathbb{E}\{H_{ti} H_{t-\Delta,i} (g'_i)^2\} \\ &+ \sum_i \sum_{j\neq i} \mathbb{E}\{H_{ti} H_{t-\Delta,j} g'_i g'_j\} \\ &\overset{a}{=} \sum_i \mathbb{E}\{H_{ti} H_{t-\Delta,i} (g'_i)^2\} \\ &+ \sum_i \mathbb{E}\{H_{ti} g'_i\} \sum_{j\neq i} \mathbb{E}\{H_{t-\Delta,j} g'_j\},\end{aligned}$$

where $\overset{a}{=}$ follows from assumption A3. Hence,

$$\begin{aligned}\mathbb{E}\{v(t)v(t-\Delta)\} &= \sum_i \mathbb{E}\{H_{ti} H_{t-\Delta,i} (g'_i)^2\} \\ &+ \sum_i \mathbb{E}\{H_{ti} g'_i\} c_i \\ &\overset{b}{=} \sum_i \mathbb{E}\{H_{ti} H_{t-\Delta,i} (g'_i)^2\} \\ &- \sum_i \mathbb{E}\{H_{ti} g'_i\} \mathbb{E}\{H_{t-\Delta,i} g'_i\},\end{aligned}$$

where $c_i = \left(\sum_j \mathbb{E}\{H_{t-\Delta,j} g'_j\} - \mathbb{E}\{H_{t-\Delta,i} g'_i\}\right)$ and $\overset{b}{=}$ follows from assumptions B1 since $\sum_j \mathbb{E}\{H_{t-\Delta,j} g'_j\} = \mathbb{E}\{v(t-\Delta)\} = 0$. At this point, let $\mathcal{E}_{t,\Delta}$ denote the event of having at least one post-synaptic firing in the interval $[t-\Delta, t]$ and $\bar{\mathcal{E}}_{t,\Delta}$ denote the event of having no post-synaptic firing in the interval $[t-\Delta, t]$. Now, if we assume an exponentially decaying filter for membrane potential with a decay coefficient of τ, we obtain[8]

$$H_{ti} = \begin{cases} e^{-\Delta/\tau} H_{t-\Delta,i} + e^{d_i/\tau} \sum_{t-\Delta<t_i<t} e^{-\frac{t-t_i}{\tau}}, & \text{if } \bar{\mathcal{E}}_{t,\Delta}, \\ e^{d_i/\tau} \sum_{t_f<t_i<t} e^{-\frac{t-t_i}{\tau}}, & \text{if } \mathcal{E}_{t,\Delta}. \end{cases} \quad (35)$$

Therefore, and by letting

$$p_{\text{fire}} = \Pr\{\text{a post-synaptic firing in} \in [t-\Delta, t]\},$$

from Equation (35) we obtain

$$\begin{aligned}\mathbb{E}\{H_{ti}\} &= (1-p_{\text{fire}}) e^{-\Delta/\tau} \mathbb{E}\{H_{t-\Delta,i}\} \\ &+ (1-p_{\text{fire}}) \mathbb{E}\{S_1\} + p_{\text{fire}} \mathbb{E}\{S_2\}, \quad (36)\end{aligned}$$

where

$$S_1 = e^{d_i/\tau} \sum_{t-\Delta<t_i<t} e^{-\frac{t-t_i}{\tau}},$$

$$S_2 = e^{d_i/\tau} \sum_{t_f<t_i<t} e^{-\frac{t-t_i}{\tau}}.$$

Furthermore, we have

$$\begin{aligned}\mathbb{E}\{H_{ti} H_{t-\Delta,i}\} &= (1-p_{\text{fire}}) e^{-\Delta/\tau} \mathbb{E}\{(H_{t-\Delta,i})^2\} \\ &+ (1-p_{\text{fire}}) \mathbb{E}\{S_1\} \mathbb{E}\{H_{t-\Delta,i}\} \\ &+ p_{\text{fire}} \mathbb{E}\{S_2\} \mathbb{E}\{H_{t-\Delta,i}\}, \quad (37)\end{aligned}$$

where we have used assumption A5. As a result, and combining Equations (35), (36) and (37) we obtain

$$\begin{aligned}\mathbb{E}\{v(t)v(t-\Delta)\} &= \sum_{i=1}^m \mathbb{E}\{(H_{t-\Delta,i})^2\} c_i \\ &- \sum_{i=1}^m (\mathbb{E}\{H_{ti} H_{t-\Delta,i}\})^2 c_i \\ &= e^{-\Delta/\tau} (1-p_{\text{fire}}) \sum_{i=1}^m \sigma_i^2 \mathbb{E}\{(g'_i)^2\}, \quad (38)\end{aligned}$$

[8] The choice of filter is made for convenience of representation only and we can extend the proof to other decaying potentials as well.

where

$$c_i = \mathbb{E}\{(g_i')^2\} e^{-\Delta/\tau}(1 - p_{\text{fire}}),$$

and

$$\sigma_i^2 = \mathbb{E}\{(H_{t-\Delta,i})^2\} - (\mathbb{E}\{H_{ti} H_{t-\Delta,i}\})^2.$$

In the above equation, both $e^{-\Delta/\tau}$ and $1 - p_{\text{fire}}$ are decreasing functions of Δ (i.e., the time interval). Therefore, the correlation is vanishing which proves the lemma.

A.3 Proof of Theorem 1

The proof is actually a direct consequence of Lemma 1 and Lemma 2: Lemma 2 makes sure that, given assumptions A3-A5, the contribution of outside traffic satisfies the assumptions about the noise term in Lemma 1. Combined with assumptions A1-A2, we can then apply the proof of Lemma 1 to prove the desired result here.

A.4 Proof of Theorem 2

To start the proof, let $e_t = H_t w$. Then, we are first interested to show that the following two problems have the same maximizer

$$\max_{w, \|w\|_2 = 1} E_1 = \sum_t \log\left(f_s(e_t)\right) \tag{39}$$

and

$$\max_{w, \|w\|_2 = 1, Hw \geq 0} E_2 = -\sum_t L(e_t), \tag{40}$$

where $L(.)$ is a "suitable" cost function, i.e. it is decreasing and $\log(f_s(x)) \leq -L(x)$. Now, the proof consists of two steps

1. Showing that both functions E_1 and E_2 are an increasing function over their domain, namely, e_t.
2. showing that $E_1 \leq E_2$.

The first part follows from the fact that

$$\frac{\partial E_1}{e_t} = \frac{f_s'(e_t)}{f_s(e_t)} \geq 0,$$

where the inequality follows from the fact that $0 \leq f_s(x) \leq 1$ and $f_s(x)$ is an increasing function of x, therefore its derivative is always positive. Additionally, since $L(x)$ is a decreasing function, E_2 is also increasing.

Furthermore, note that since we have selected $L(x)$ to be less than $-\log(f_s(x))$, then we will have

$$E_1 \leq E_2.$$

All this results in the fact that the argmax of function E_2 will also maximize E_1.

Now, given that the objective functions for both Problem (39) and Problem (40) is increasing, the maximizer of both are at the boundaries. Therefore, in order to solve the ML problem given in Equation (13), we can focus on solving the potentially simpler problem, called *Problem II* and given by Equation (8). This concludes the proof.

References

Baldassi C, Braunstein A, Brunel N, Zecchina R (2007) Efficient supervised learning in networks with binary synapses. BMC Neuroscience 8(Suppl 2):S13

Bertotti G, Velychko D, Dodel N, Keil S, Wolansky D, et al (2014) A cmos-based sensor array for in-vitro neural tissue interfacing with 4225 recording sites and 1024 stimulation sites. In: Biomedical Circuits and Systems Conference (BioCAS), 2014 IEEE, IEEE, pp 304–307

Brown EN, Kass RE, Mitra PP (2004) Multiple neural spike train data analysis: state-of-the-art and future challenges. Nature neuroscience 7(5):456–461

Buzsáki G (2004) Large-scale recording of neuronal ensembles. Nature neuroscience 7(5):446–451

Chiang AS, Lin CY, Chuang CC, Chang HM, Hsieh CH, Yeh CW, Shih CT, Wu JJ, Wang GT, Chen YC, et al (2011) Three-dimensional reconstruction of brain-wide wiring networks in drosophila at single-cell resolution. Current Biology 21(1):1–11

Dale H (1935) Pharmacology and nerve-endings. J Royal Society of Medicine 28(3):319–332

Gerhard F, Kispersky T, Gutierrez GJ, Marder E, Kramer M, Eden U (2013) Successful reconstruction of a physiological circuit with known connectivity from spiking activity alone. PLoS computational biology 9(7):e1003,138

Gerstner W, Kistler WM (2002) Spiking neuron models: Single neurons, populations, plasticity. Cambridge university press

Goldstein T, Studer C, Baraniuk R (2014) A field guide to forward-backward splitting with a fasta implementation. arXiv preprint arXiv:14113406

Grewe BF, Langer D, Kasper H, Kampa BM, Helmchen F (2010) High-speed in vivo calcium imaging reveals neuronal network activity with near-millisecond precision. Nature methods 7(5):399–405

Herrera CG, Adamantidis AR (2015) An integrated microprobe for the brain. Nature Biotechnology 33(3):259–260

Jaggi M, Smith V, Takác M, Terhorst J, Krishnan S, Hofmann T, Jordan MI (2014) Communication-efficient distributed dual coordinate ascent. In: Advances in Neural Information Processing Systems, pp 3068–3076

Karbasi A, Salavati AH, Vetterli M (2015) Learning network structures from firing patterns. In: International Conference on Acoustics, Speech and Signal Processing

Khodagholy D, Gelinas JN, Thesen T, Doyle W, Devinsky O, Malliaras GG, Buzsáki G (2014) Neurogrid: recording action potentials from the surface of the brain. Nature neuroscience

Kim S, Putrino D, Ghosh S, Brown EN (2011) A granger causality measure for point process models of ensemble neural spiking activity. PLoS computational biology 7(3):e1001,110

Maass W, Schmitt M (1999) On the complexity of learning from spiking neurons with temporal coding. Information and Computation 153(1):26–46

Memmesheimer RM, Rubin R, Ölveczky BP, Sompolinsky H (2014) Learning precisely timed spikes. Neuron 82(4):925–938

Mishchenko Y, Vogelstein JT, Paninski L, et al (2011) A "b"ayesian approach for inferring neuronal connectivity from calcium fluorescent imaging data. The Annals of Applied Statistics 5(2B):1229–1261

Mizuseki K, Sirota A, Pastalkova E, Buzsáki G (2009) Theta oscillations provide temporal windows for local circuit computation in the entorhinal-hippocampal loop. Neuron 64(2):267–280

Mizuseki K, Sirota A, Pastalkova E, Diba K, Buzski G (2013) Multiple single unit recordings from different rat hippocampal and entorhinal regions while the animals were performing multiple behavioral tasks. CRCNS org

Paninski L (2004) Maximum likelihood estimation of cascade point-process neural encoding models. Network: Computation in Neural Systems 15(4):243–262

Perin R, Berger TK, Markram H (2011) A synaptic organizing principle for cortical neuronal groups. Proceedings of the National Academy of Sciences 108(13):5419–5424

Pillow JW, Shlens J, Paninski L, Sher A, Litke AM, Chichilnisky E, Simoncelli EP (2008) Spatio-temporal correlations and visual signalling in a complete neuronal population. Nature 454(7207):995–999

Plaza SM, Scheffer LK, Chklovskii DB (2014) Toward large-scale connectome reconstructions. Curr Opin Neurobiology 25:201–210

Ramirez AD, Paninski L (2014) Fast inference in generalized linear models via expected log-likelihoods. Journal of computational neuroscience 36(2):215–234

Schur J (1911) Bemerkungen zur theorie der beschrankten bilinearformen mit unendlich vielen veranderlichen. Journal fur die reine und Angewandte Mathematik 140:1–28

Stevenson IH, Rebesco JM, Hatsopoulos NG, Haga Z, Miller LE, Körding KP (2009) Bayesian inference of functional connectivity and network structure from spikes. Neural Systems and Rehabilitation Engineering, IEEE Transactions on 17(3):203–213

Van Bussel F, Kriener B, Timme M (2011) Inferring synaptic connectivity from spatio-temporal spike patterns. Frontiers in computational neuroscience 5

Watts DJ, Strogatz SH (1998) Collective dynamics of small-world networks. Nature 393(6684):440–442

Wright SJ, Nowak RD, Figueiredo MA (2009) Sparse reconstruction by separable approximation. IEEE Transactions on Signal Processing 57(7):2479–2493

Zaytsev Y, Morrison A, Deger M (2015) Reconstruction of recurrent synaptic connectivity of thousands of neurons from simulated spiking activity. Journal of Computational Neuroscience 39(1):77–103, DOI 10.1007/s10827-015-0565-5, URL http://dx.doi.org/10.1007/s10827-015-0565-5